X-ray scattering study of the Ge(001):Te(1×1) surface structure

Osami Sakata
Department of Materials Science and Engineering and Materials Research Center, Northwestern University, Evanston, Illinois 60208

P. F. Lyman
Department of Physics, University of Wisconsin-Milwaukee, Wisconsin, 53201

B. P. Tinkham and D. A. Walko
Department of Materials Science and Engineering and Materials Research Center, Northwestern University, Evanston, Illinois 60208

D. L. Marasco
Department of Physics and Astronomy and Materials Research Center, Northwestern University, Evanston, Illinois 60208 and Materials Science Division, Argonne National Laboratory, Argonne, Illinois 60439

T.-L. Lee
Department of Materials Science and Engineering and Materials Research Center, Northwestern University, Evanston, Illinois 60208

M. J. Bedzyk*
Department of Materials Science and Engineering and Materials Research Center, Northwestern University, Evanston, Illinois 60208 and Materials Science Division, Argonne National Laboratory, Argonne, Illinois 60439

(Received 6 March 2000)

The 1×1 surface structure of Te adsorbed on Ge(001) was studied by analyzing the x-ray scattered intensity along several surface crystal truncation rods (CTR). The results were compared to simulations corresponding to the bridge, top, antibridge, and hollow site models. Te at the bridge site was in best agreement. More complex surface models based on modifications of Te at the bridge site were then compared to the data with the missing-row model being in better agreement than the zigzag model. Finally, the CTR data were used to refine the structural parameters of the missing row model.

INTRODUCTION

Tellurium has proven to be an effective surfactant in forming sharp interfaces in Ge/Si hetero-epitaxial structures grown by molecular beam epitaxy (MBE).[1] To understand this growth mechanism on an atomic scale, structural parameters, such as adsorption sites and bondlengths for both Te on Si(001) and Te on Ge(001) are important prerequisites. In a scanning tunneling microscopy (STM) study of the Si(001):Te(1×1) surface,[2] a local structural model was proposed wherein the Te atoms were located at substitutional (i.e., bridge) sites. Although the local structure was 1×1, this study observed a modified long-range order, in which missing rows of Te occurred at random intervals having an average spacing of 5–6 rows, presumably to relieve surface compressive strain imposed by the Si lattice. Using surface extended x-ray absorption fine structure (SEXAFS) and x-ray standing waves (XSW),[3] Burgess *et al.* determined the Te-Si bondlength for the Si(001):Te(1×1) surface and also concluded that the Te adsorption site was indeed substitutional (i.e., bridge site). The missing-row model proposed in the STM study is also consistent with the observed streaky 1×1 low energy electron diffraction (LEED) pattern,[2] although such streaks also can be explained by a mixture of 1×1 and 2×1 domains.[4]

Using XSW and LEED, Lyman *et al.*[5] made an atomic scale study of the Te/Ge(001) surface. For the 1 ML Te/Ge(001) surface the (004) and (022) XSW coherent positions triangulated the Te positions and found them to be consistent with a twofold bridge site. The observed reduction in the XSW (022) coherent fraction was shown to agree with the expected Te lateral displacements from the bridge-sites in the missing row model [Fig. 1(a)] due to the misfit between the Ge and Te overlayer. In addition, the streakiness of the corresponding 1×1 LEED pattern was explained by missing rows at irregular intervals similar to the local structure of the Te/Si(001) surface seen by Yoshikawa *et al.*[2] using STM. Takeuchi[6] recently reported possible atomic scale structural models for the 1 and 0.8 ML covered Te surfaces on Ge(001) based on first-principles total energy calculations. These structural models consider Te at the bridge, top, antibridge, hollow, and modified-bridge sites. Of the high-symmetry sites, Te at the bridge site is energetically most favorable, but the energy can be lowered further by allowing a small shift of the Te atoms from 1×1 symmetry (''zigzag'' model [Fig. 1(b)]). The study also calculated energies for the missing Te row model [see, for example, Fig. 1(a)], allowing relaxation of the Te atoms off the bridge sites. The energy difference between the two models, ''zigzag'' and missing row, was not reported due to difficulties in comparing the energies for the two models which used different size clusters.[7] Presently, no definitive structural models have been proposed for Te/Si(001) or Te/Ge(001).

Herein, we report on the Ge(001):Te(1×1) structure us-

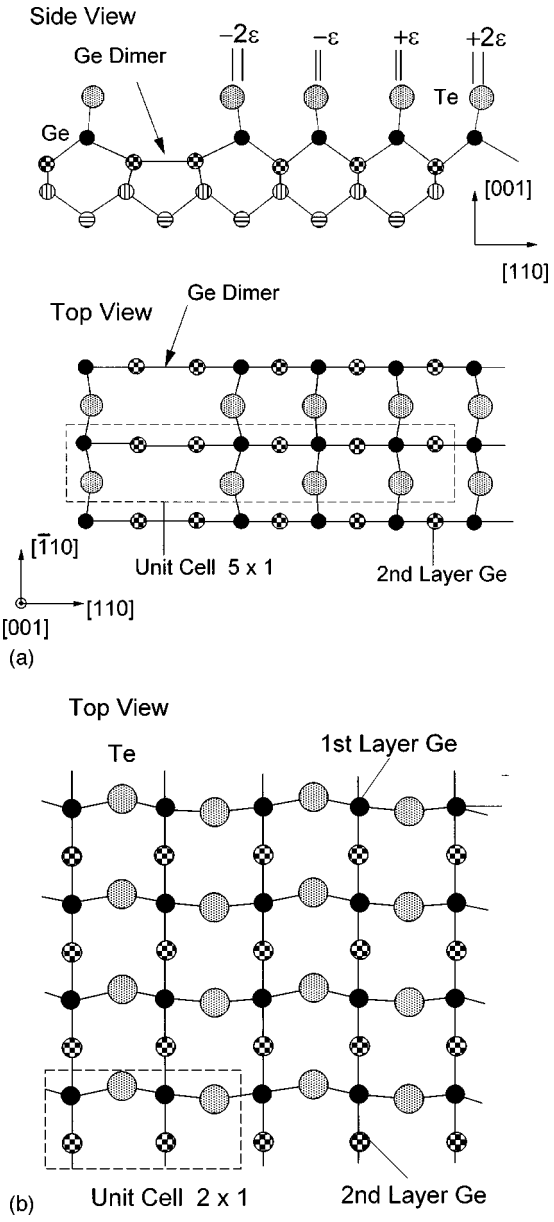

FIG. 1. Te missing row model (a) and Te zigzag model (b). Note that the Ge dimer directions in (a) differ by 90° from the model proposed by Takeuchi (Ref. 6).

ing x-ray crystal truncation rod (CTR) measurements.[8] Our experimental intensity profiles will be compared to calculated profiles based on the bridge, top, antibridge and hollow sites. We will further consider slightly distorted Te(1×1) surface models, namely the zigzag model and the aforementioned missing row model. Finally, we will refine the Te missing row model to determine surface relaxation for Te atoms and the top Ge atomic layers. Comparatively speaking, x-ray scattering measurements are more sensitive to disorder such as relaxation and vacancies, while XSW measurements give the exact adsorbate position with respect to the bulk atomic planes.

POSSIBLE Te ADSORPTION SITES

We will consider the four possible high-symmetry Te adsorption sites on the Ge(001) unreconstructed surface,

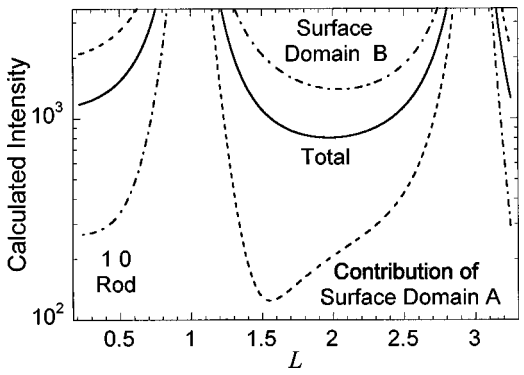

FIG. 2. Calculated intensities along the 1 0 L rod from a Te/Ge (001) surface with Te at the bridge site. No germanium surface relaxation is assumed. Surface domain B is one atomic step height above surface domain A.

namely the bridge, hollow, top, and antibridge sites. The bridge site is the Ge substitutional position. The top, antibridge, and hollow sites are directly above the Ge site in the first, second, and third atomic layers, respectively. We will not make any assumptions about the bond directions between the adsorbed Te atom and its nearest neighbors, but will instead attempt to determine the adsorption site from the x-ray diffraction data.

For an ideally terminated (001) Ge surface, we employ a tetragonal surface unit cell which is related in direct space to the conventional cubic unit cell (denoted with subscript c) of the bulk; $\mathbf{a}=[100]=1/2[110]_c$, $\mathbf{b}=[010]=1/2[-110]_c$, $\mathbf{c}=[001]=[001]_c$. In reciprocal space, $(100)=(110)_c$, $(010)=(-110)_c$, and $(001)=(001)_c$. The cubic coordinates are in units of the germanium lattice constant (5.658 Å) and hence $a=b=4.001$ Å and $c=5.658$ Å. For the ideally terminated Ge(001) surface, there are two surface domains (terraces) separated by a height difference of one atomic layer; the two Ge dangling bonds are directed along the [101] and [−101] on surface domain A and along the [011] and [0−11] on surface domain B. A given Te adsorption site is located in different positions with respect to the bulk lattice for the two different surface domains. For surface domain A, the bridge site is $(0,0,Z_0)$, the hollow site is $(0,1/2,Z_0)$, the top site is $(1/2,0,Z_0)$, and the antibridge site is $(1/2,1/2,Z_0)$. While for surface domain B, the bridge site is $(0,1/2,Z_0+1/4)$, the hollow site is $(1/2,1/2,Z_0+1/4)$, the top site is $(0,0,Z_0+1/4)$, and the antibridge site is $(1/2,0,Z_0+1/4)$. These differences in coordinates will, of course, affect the phases of the scattered waves. The x-ray scattering intensity is proportional to the square of the modulus of the structure factor, which in turn is the sum of the structure factors for the bulk and surface layer.[8] As can be seen in Fig. 2, the calculated scattering intensity along the 1 0 L rod from surface domain A with Te bridge sites has a very different profile than that of surface domain B. [For these calculations, we used the XSW (Ref. 5) obtained value of $Z_0=0.267$ (in units of the [001] spacing).] We averaged the two squares of the structure factors for surface A termination and for surface B termination, since both surface domains exist in equal proportion. The contrast of the two curves demonstrates the great sensitivity of CTR measurements to the surface structure.

For surface domain A, the bridge and hollow sites sit on

the (100) planes and the top and antibridge sites are halfway between the (100) planes. For surface domain *B*, the bridge and top sites are on the (100) planes and the hollow and antibridge sites are in the middle of the planes. This implies that the bridge and antibridge sites are on the (110) planes in surface *A* while they sit halfway between these planes in surface domain *B*, and vice versa for the hollow and top sites. Consequently, x-ray intensity profiles along $1\,0\,L$ will be different for all four sites. The $1\,1\,L$ scans would provide the same profile for the bridge and antibridge sites, and the same profile for the hollow and top sites.

SAMPLE PREPARATION AND X-RAY CRYSTAL TRUNCATION ROD MEASUREMENTS

The experiments were carried out in an ultrahigh vacuum (UHV) surface chamber that is part of an x-ray diffractometer[9,10] at the 5ID-C station on the DND undulator beamline at the Advanced Photon Source (APS). The UHV chamber has surface preparation capabilities including ion sputtering, annealing, and solid source MBE, as well as surface analysis via LEED, Auger electron spectroscopy (AES), x-ray fluorescence, x-ray photoelectron spectroscopy, XSW, SEXAFS and surface x-ray scattering. There is also a sample introduction and sample storage UHV chamber attached to the main chamber. The base pressure was 2.5×10^{-10} Torr for the main chamber and better than 1×10^{-9} Torr for the sample storage chamber. Lyman *et al.*[9] reported earlier on the design of the main chamber coupled to a psi goniometer.

The sample was prepared by a similar method as previously reported for Ge(001):Te(1×1).[5] A $14\times10\times3$ mm^3 Ge(001) substrate was degreased using acetone and methanol, mounted on a molybdenum holder and then introduced into the main chamber via the storage chamber. The substrate was outgassed for 10 min at 970 K and sputtered for 1 h at 720 K using 1 keV Ar^+ ions with a differentially pumped ion gun. The substrate was then annealed for 10 min at 960 K followed by cooling at 2°/s. The annealing temperature used was below the Ge roughening temperature of 1020 K.[11] This cycle was repeated three times, resulting in a sharp, two-domain 2×1 LEED pattern. Te was deposited onto the Ge substrate from an effusion cell operated at ~570 K with the sample held at ~540 K. The sample was then held at ~540 K for 10 min after the Te shutter was closed and the Knudsen cell power turned off. We observed a 1×1 LEED pattern with streaks between the 00 and 10 spots. To remove any loosely bound Te on the surface, we heated the sample for 20 min at 690 K. This process reduced the background intensity in the LEED pattern, but the streaks remained in the pattern (Fig. 3). This indicates that the surface had 1×1 long-range order but was locally disordered.

The 18.0 keV incident x-ray beam was prepared by using the third harmonic of the undulator and the L-N_2 cooled double crystal Si(111) beamline monochromator. A pair of beamline horizontally deflecting mirrors were set to reject harmonics and to horizontally focus the monochromatic beam. At the sample position the beam size was 1.2 mm in the vertical direction and 0.6 mm in the horizontal. In the scattering direction the slits on the detector arm were set to give an angular resolution of 0.85 mrad in the vertical direction and 1.7 mrad in the horizontal. We recorded scattered

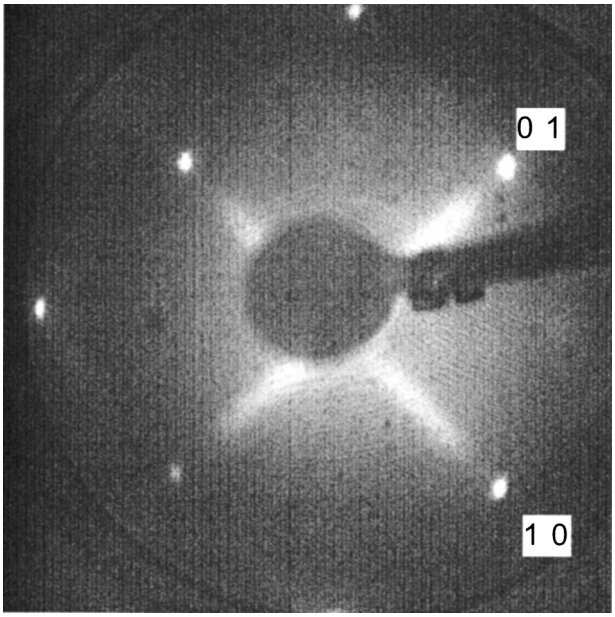

FIG. 3. LEED pattern observed from the Ge(001):Te(1×1) surface with strong streaks along the [10] and [01] directions at an electron beam energy of 35 eV.

intensities along the $10\,L$, $11\,L$, and $30\,L$ crystal truncation rods with the incident angle fixed at 0.5°. (The critical angle for total external reflection of 18 keV x-rays reflecting from Ge is 0.14°.) The net counts at each point along a CTR were obtained from a transverse scan through the CTR with subtraction of a linear background.[12] One of the weakest intensities at $L=1.75$ in the $1\,0\,L$ scan was 2.1×10^4 counts/s/mm^2. The Lorentz, polarization, and geometrical corrections were then used to convert the integrated intensity to a measured structure factor $|F_{\rm obs}|$.[12–15]

COMPARISON BETWEEN THE EXPERIMENTAL AND CALCULATED STRUCTURE FACTORS

We compared the measured structure factor $|F_{\rm obs}|$ to model-based calculated structure factor $|F_{\rm cal}|$' values that include a roughness contribution ($|F_{\rm cal}|\times F_r$). The roughness factor F_r was introduced by Robinson [8] and is expressed as

$$F_r=(1-\beta)/[1+\beta^2-2\cos\{2\pi(L-N_B)/N_L\}]^{1/2}, \quad (1)$$

where β is expressed in terms of the rms roughness σ_r as

$$\beta=[-c/n+\{(c/n)^2+4\sigma_r^2\}^{1/2}]^2/4\sigma_r^2. \quad (2)$$

$n(=4)$ is the number of Ge atomic layers in the unit cell. For the $1\,0\,L$, $1\,1\,L$, and $3\,0\,L$, values of N_B are set to 1, 2, and 1 and those of N_L are 2, 4, and 2, respectively. We fit the structure factors for the $1\,0\,L$, $1\,1\,L$, and $3\,0\,L$ scans together with calculated ones based on Te occupying the bridge, hollow, top, and antibridge site (Fig. 4).[16] At this initial stage in the analysis the Te vertical position was fixed at the position obtained from the XSW experiment,[5] and the Ge surface atoms were given bulklike positions. In addition, we set the Te coverage at 0.74 ML based on a Rutherford backscattering spectroscopy (RBS) measurement. The rms vibrational amplitudes were approximated as being isotropic and set at $(\langle u^2\rangle_{\rm Te})^{1/2}=0.13$ Å and $(\langle u^2\rangle_{\rm Ge})^{1/2}=0.10$ Å. The

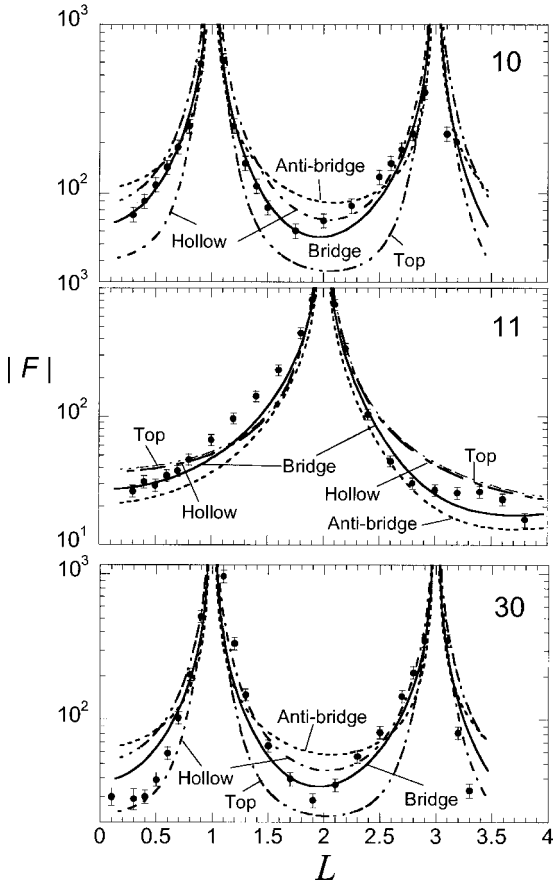

FIG. 4. Comparison of the experimental structure factors and the calculated structure factors (relative values including roughness) based on the bridge, hollow, top, and antibridge site models. Filled circles represent the experimental data.

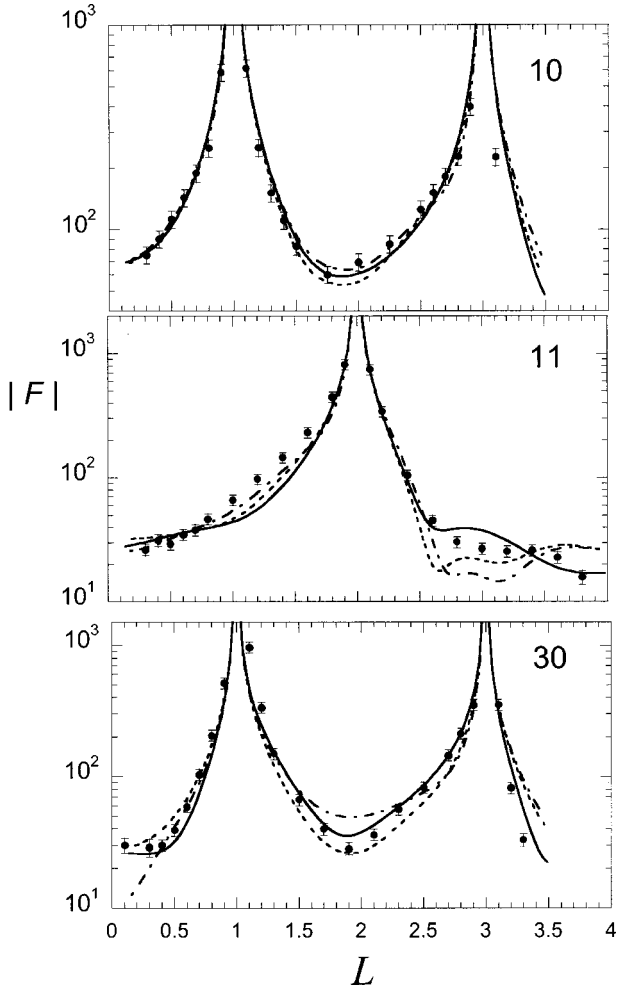

FIG. 5. Experimental (filled circles) and calculated (line) structure factors (relative values including roughness) for the Te missing-row model (dashed line) and the Te zigzag model (dot-dashed line). The refined missing-row model (solid line) includes surface relaxations for the Te and Ge atom layers.

former value was also used in Ref. 5 and the latter corresponds to bulk Ge at room temperature. The two free parameters of these least-squares fits are surface roughness and a scale factor. Each of these parameters was forced to be equivalent for all three CTR fits of a given model to the data. χ^2 values obtained were 2.34, 3.26, 7.05, and 11.1 for the Te bridge, hollow, top, antibridge site models, respectively. Based on this initial analysis (shown in Fig. 4) the hollow, top, and antibridge site models were ruled out and the bridge site model was found to be most favorable with a surface roughness of $\sigma_r = 2.1$ Å.

To refine this model, we further compared the experimental with the calculated structure factors that are based on the atomic configurations given in Ref. 7 for the Te missing row (Fig. 3 in Ref. 6) and the Te zigzag model [Fig. 1(b)]. These two models are modified bridge site models. The 5×2 Te missing row model of Ref. 6 is very similar to the 5×1 shown in Fig. 1(a) except for the position and orientation of the Ge dimer in the missing Te row. This 5×2 model consists of a Te layer with 8 Te atoms and 5 Ge layers with 10 Ge atoms per layer in the unit cell. The 2×1 Te zigzag model shown in Fig. 1(b) is composed of a Te layer with 2 Te atoms and 6 Ge layers with 2 Ge atoms per layer. Figure 5 shows the fitted curves based on these two models together with the experimental structure factors. As before, the free parameters used in the χ^2 fits are the surface roughness and the scale factor. The χ^2 values attained are 1.94 and 2.66 for the Te missing row and zigzag models, respectively. Thus the CTR results favor the missing row model.

SURFACE RELAXATION OF Ge(001):Te(1×1)

The predicted XSW coherent fractions based on the atomic configurations given in Ref. 7 for the Te missing row and the vibrational amplitude of $(\langle u^2\rangle_{\mathrm{Te}})^{1/2} = 0.13$ Å are $f(004)_c = 0.84$ and $f(022)_c = 0.87$. The XSW-measured $(022)_c$ coherent fraction (0.77) is much lower than this prediction. To explain the lower coherent fraction for the $(022)_c$, we introduce symmetric displacements of Te lateral positions [expressed as ε and 2ε in Fig. 1(a)]. The value of ε is $0.058a$. Finally, we fit two Te missing row models (*A* and *B*) to the CTR data to refine the vertical displacements of the Te atom layer and the first four Ge atom layers. Model *A* is shown in Fig. 1(a). Model *B* differs from model *A* by having its Ge dimers that form along the missing row originate from the first Ge layer instead of the second layer. Consequently, the Ge dimer bond for model *B* is perpendicular to the direction of the Te displacements and model *B* is $p(5\times2)$. We

also used the RBS measured Te coverage (0.74 ML).[17] The isotropic vibrational amplitudes used in the fit were again $(\langle u^2\rangle_{\mathrm{Te}})^{1/2}=0.13$ Å and $(\langle u^2\rangle_{\mathrm{Ge}})^{1/2}=0.10$ Å. After allowing vertical relaxation (and using the value of the lateral displacements predicted from the XSW measurements), the CTR χ^2 are reduced to 1.25 and 1.49 for model *A* and *B*, respectively. The fitted curves for model A are shown in Fig. 5 as solid lines. In this model, the displacement of the Te atomic layer along the *Z* direction from the bulk Ge position is +0.105 Å, where + sign stands for atoms shifted outwards. The first through fourth Ge atomic layers are shifted vertically by 0.022, −0.025, −0.042, and −0.014 Å, respectively, from the bulk Ge positions. The Te-Ge bond length is 2.54 Å and 2.51 Å, for the 2ε displacement Te and ε displacement Te, which is comparable to the sum (2.54 Å) of Pauling tetrahedral atomic radii.[18] The Te position agrees to within 0.006 Å with the XSW result.[5] The obtained surface roughness is 2.1 Å. The Ge dimers are located 0.060 Å below the bulk Ge position and the fitted Ge dimer bondlength is 2.91 Å. The distance from a Ge dimer atom to its closest Ge atom below the 2ε displacement Te is 2.99 Å. These lengths are much larger than the bulk Ge-Ge bondlength (2.45 Å).

Thus, as we have seen, CTR, XSW, and theory for Te/Ge(001), as well as STM of Te/Si(001),[2] all agree with the missing row model. The principal features of the LEED patterns also agree with this model (Fig. 3). Specifically, the streaking in the (00)–(10) directions is consistent with the missing row model, as pointed out by Yoshikawa[2] and Lyman.[5] The streaks are also associated with the misfit between the substrate and the Te overlayer. However, there are several unexplained features of the LEED pattern, and the precise atomic origin of the streaking is not well established. Streaky and diffuse LEED patterns may result from interference between two surface superstructures,[19] in particular, similar streaking was observed for the related Te/Si(001) system as the surface transformed from 1×1 to 1×2 symmetry.[4] Our LEED pattern was broadly peaked near (but not exactly at) the {0, 1/2} positions, as was that of Ref. 4. In any event, it is clear that good long-range order exists along the Te rows, but a distribution of spacings occur in-plane but perpendicular to the rows.

In summary, we compared the experimental CTR data for the Ge(001):Te(1×1) surface with the four different Te adsorption site models. The bridge site was found most favorable. Two modified bridge site models were also examined. The model that best agrees with the CTR data is the missing row model. We finally estimated the vertical displacement of the top-five atom layers.

ACKNOWLEDGMENTS

We thank N. Takeuchi for providing the atomic positions from his first-principles calculation and for valuable discussion. We also thank P. Baldo for acquiring the RBS spectra. This work was supported by the U.S. Department of Energy under Contract Nos. DE-F02-96ER45588 to NU and W-31-109-ENG-38 to Argonne National Laboratory, and by the National Science Foundation under Nos. DMR-9632593, 9973436, CHE-9810378, and DMR-9632472 to NU. DND-CAT was partially supported by the State of Illinois under Contract No. IBHE HECA NWU 96.

*Author to whom all correspondence should be addressed.

[1] S. Higuchi and Y. Nakanishi, Surf. Sci. **254**, L465 (1991).
[2] S. A. Yoshikawa, J. Nogami, C. F. Quate, and P. Pianetta, Surf. Sci. **321**, L183 (1994).
[3] S. R. Burgess, B. C. C. Cowie, S. P. Wilks, P. R. Dunstan, C. J. Dunscombe, and R. H. Williams, Appl. Surf. Sci. **104/105**, 152 (1996).
[4] T. Ohtani, K. Tamiya, Y. Takeda, T. Urano, and S. Hongo, Appl. Surf. Sci. **130–132**, 112 (1998).
[5] P. F. Lyman, D. L. Marasco, D. A. Walko, and M. J. Bedzyk, Phys. Rev. B **60**, 8704 (1999).
[6] N. Takeuchi, Surf. Sci. **426**, L433 (1999).
[7] Private communication with N. Takeuchi.
[8] I. K. Robinson, Phys. Rev. B **33**, 3830 (1986).
[9] P. F. Lyman, D. T. Keane, and M. J. Bedzyk, in *Synchrotron Radiation Instrumentation,* edited by Ernest Fontes, AIP Conf. Proc. No. 417 (AIP, Woodbury, NY, 1997), pp. 10–14.
[10] O. Sakata *et al.* (unpublished).
[11] A. D. Johnson, C. Norris, J. W. M. Frenken, H. S. Derbyshire, J. E. MacDonald, R. G. Van Silfhout, and J. F. Van Der Veen, Phys. Rev. B **44**, 1134 (1991).
[12] For example, R. Feidenhans'l, Surf. Sci. Rep. **10**, 105 (1989); I. K. Robinson, in *Handbook on Synchrotron Radiation,* edited by G. Brown and D. E. Moncton (Elsevier Science Publishers B.V., New York, 1991), Vol. 3, Chap. 7.
[13] The Lorentz factor (Ref. 14) and the polarization factor (Refs. 14 and 15) used for the psi diffractometer are $1/(\sin\delta\cos\mu)$ and $1-\sin^2\nu\cos^2\delta$, respectively. Here δ around the horizontal axis and ν around the vertical axis are angles for the detector and μ around the vertical axis is for sample rotation.
[14] E. Vlieg, J. Appl. Crystallogr. **31**, 198 (1998).
[15] K. W. Evans-Lutterodt and M.-T. Tang, J. Appl. Crystallogr. **28**, 318 (1995).
[16] Calculated 1 1 *L* profiles in Fig. 4 are not exactly the same for the bridge and antibridge sites, and for the hollow and top sites unlike previously mentioned. The disagreements arise from slight differences in the scale factor and surface roughness obtained by the fits including the 1 0 *L* and 3 0 *L* scans.
[17] To explain to 0.74 ML Te coverage, we assume that the two domains with the Te missing row structure occupy 92.5% of the measured surface. It is assumed for simplicity that the remainder is occupied by an unreconstructed Ge surface.
[18] L. Pauling and M. L. Huggins, Z. Kristallogr. **87**, 205 (1934).
[19] R. L. Gerlach and T. N. Rhodin, Surf. Sci. **17**, 32 (1969).